

Observing Correlated Production of Defects-Antidefects in Liquid Crystals

Sanatan Digal, Rajarshi Ray, and Ajit M. Srivastava

Institute of Physics, Sachivalaya Marg, Bhubaneswar 751005, India

Abstract

We present observation of strength one defects and antidefects formed in isotropic-nematic phase transition in nematic liquid crystals using a cross-polarizer setup. We measure the width σ of the distribution of *net* winding number in two dimensional regions, each containing an average of 10 defects and antidefects. We find $\sigma = 1.19 \pm 0.04$, in good agreement with the value 1.02 or 1.26 (for triangular or square domains) predicted by the Kibble mechanism for defect production. We also describe a novel technique to determine the director distribution in such observations.

PACS numbers: 61.30.Jf, 98.80.Cq, 64.70.Md

Study of topological defects is one of the areas in physics which is highly interdisciplinary in nature. This has led to a valuable interplay of ideas from different branches of physics. For example, the first theory of formation of topological defects, formulated by Kibble [1] in the context of the early Universe, found experimental verification of some of its aspects in certain condensed matter systems [2–5]. One of the predictions of the Kibble mechanism, namely the average defect density, has been experimentally verified in liquid crystal systems [2] as well as in superfluid helium [4]. In this paper, we present experimental verification of a qualitatively different prediction of the Kibble mechanism, namely correlations in the production of defects and antidefects.

In Kibble mechanism, defects form due to a domain structure arising after a phase transition. For example, in a spontaneous symmetry breaking transition of a global $U(1)$ symmetry, with a complex order parameter Ψ , the order parameter space is a circle S^1 . Phase θ of Ψ can vary spatially and domains are characterized by roughly uniform value of θ . θ varies randomly from one domain to another, and varies with least gradient in between adjacent domains (the *geodesic rule*). There are string defects here characterized by non-zero winding of θ around the string. The probability of string formation (in 2 dimensions) can be estimated by considering a junction of three domains. If the values of θ in these three domains are α_1 , α_2 , and α_3 , then it is easy to show that a non-trivial winding around the junction will result if one of the angles, say α_1 lies in the arc formed by the opposite points of the other two angles (α_2 and α_3) on the circle S^1 . Average angular span of this arc is $\pi/2$ (smallest being zero and largest being π). As α_1 can lie anywhere between 0 and 2π , the probability of having a winding at the junction is $1/4$.

For uniaxial nematic liquid crystals (NLC) the orientation of the order parameter is given by a unit vector (with opposite directions identified) called as the director. Order parameter vanishes in the high temperature isotropic phase. In the low temperature nematic phase, (rod like) molecules align locally, leading to non zero magnitude of the order parameter. This leads to the order parameter space being $RP^2(\equiv S^2/Z_2)$. There are string defects with winding $1/2$ corresponding to rotation of the director by π around the string.

There is an important prediction for defect distribution, arising from the Kibble mechanism, which is qualitatively different from the prediction of average density. Consider a string formed at the junction of three domains. Given this, the probability of formation of an antistring in the neighboring region increases since part of the (anti)winding of θ is already present, and one only needs to have right θ value, say, in a fourth domain adjacent to the other three domains. This conclusion, that the Kibble mechanism leads to certain correlation between formation of a defect and an antidefect, is valid for other types of defects as well. The effect of this correlation is the following [6]. Consider a closed curve of perimeter L going through L/ξ number of elementary domains (where ξ is the domain size). As θ varies randomly from one domain to another, one essentially is dealing with a random walk problem with the average step size for θ being $\pi/2$ (largest step is π and smallest is zero). Thus, the net winding number of θ around L will be distributed about zero with a typical width given by $\sigma = \frac{1}{4}\sqrt{\frac{L}{\xi}}$. For simplicity, consider the two dimensional region to be a square with its area $A = (L/4)^2$. If we take the elementary domains to be equilateral triangles, then, with the probability of defects per domain being $1/4$, we can rewrite σ in terms of average value of net number of defects n_t in this area as

$$\sigma = \frac{1}{4}(16 \sqrt{3} n_t)^{1/4} \simeq 0.57 n_t^{1/4} \quad (1)$$

If one takes elementary domains to be square shaped, then predicted value of σ is about $0.71 n_t^{1/4}$. (One may have a mixture of domains of various shapes and sizes in a local region. It is not known what should be the correct distribution of domains. Thus we simply take all domains to be roughly similar.) This equation reflects the correlation between the production of defect and antidefect. In the absence of any correlations, net defect number will not be as suppressed, and will follow Poisson distribution with $\sigma \simeq \sqrt{n_t}$.

NLCs provide an excellent system to test this prediction of the Kibble mechanism, as a simple cross-polarizer setup can identify the winding number of the defect [7]. [We mention here, that certain other techniques for determining the director distribution [8] may not be suitable for observing an evolving defect distribution.] Due to birefringence of NLC, when the liquid crystal sample is placed between a cross polarizer setup, then regions where director is either parallel, or perpendicular, to the electric field \vec{E} , the polarization is maintained resulting in a dark brush. At other regions, the polarization changes through the sample, resulting in a bright region. This implies that for a defect of strength s , one will observe $4s$ number of dark brushes. If the cross-polarizer setup is rotated then brushes will rotate in the same (opposite) direction for positive (negative) windings.

We now describe our experiment. We observed isotropic-nematic (I-N) transition in a tiny droplet (size ~ 2 -3 mm) of NLC 4'-pentyl-4-biphenyl-carbonitrile (98% pure, purchased from Aldrich Chem. Co., Milwaukee, USA). The sample was placed on a clean glass slide and was heated using an ordinary lamp. The I-N transition temperature is about 35.3 °C. Our setup allowed the possibility of slow heating, and cooling (by changing the distance of the lamp from the sample). We observed the defect production very close to the transition temperature (in some cases we had some isotropic bubbles co-existing with the nematic layer containing defects). We used a Leica, DMRM microscope with 20x objective, a CCD camera, a photographic SLR camera, and a cross-polarizer setup for the observations. Phase transition process was recorded on a standard video cassette recorder. The images were later photographed directly from a television monitor by replaying the cassette and choosing appropriate events carefully.

The I-N transition is of first order. We find that when the transition proceeds via nucleation of bubbles, one primarily gets long horizontal strings which are not suitable for our analysis. We selected those events where the transition seems to occur uniformly on a thin layer on top of the droplet (possibly due to faster cooling from contact with air). Depth of field of our microscope was about 20 microns. All the defects in the field of view were well focussed suggesting that they formed in a thin layer, especially since typical inter-defect separation was about 30 - 40 microns. (For us, the only thing relevant is that the layer be effectively two dimensional over distances of order of typical inter-defect separation). Also, the transition happened over the entire observation region roughly uniformly, suggesting that a process like spinodal decomposition may have been responsible for the transition. This resulted in a distribution of strength one defects as shown in the photographs in Fig.1. Points from which four dark brushes emanate correspond to defects of strength ± 1 .

Top picture in Fig.1 was taken with the photographic camera. It clearly shows the point like nature of the defects corresponding to crossing of brushes. We analyze the picture shown

at the bottom in Fig.1 (which was taken from the video recording of the transition) where density of defects is much larger. Due to resolution limitation, or due to rapidly evolving director configuration, the crossings here do not appear as point like. The sign of the winding number could not be determined in our present experimental setup using rotation of polarizers. This becomes very difficult due to the fact that the transition proceeded rather fast leading to extremely rapid evolution of defect distribution.

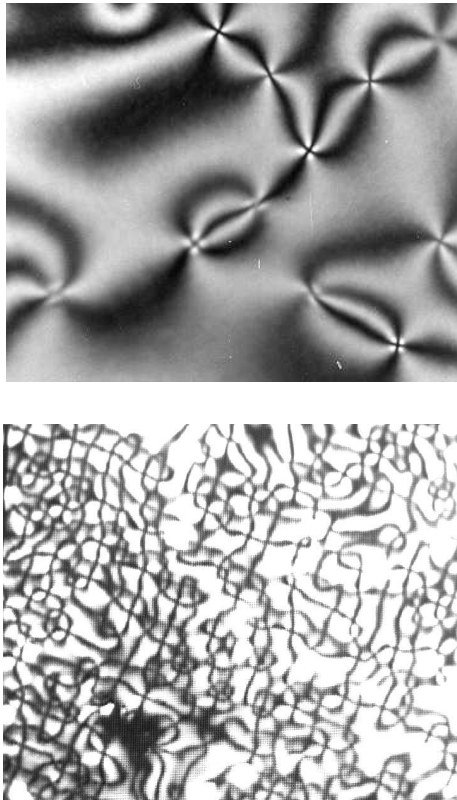


FIG. 1. Pictures of defect distribution observed using cross-polarizers in I-N transition. Dark brushes connect defect-antidefect pairs and crossing of brushes correspond to defects with windings ± 1 . Size of each image is about $0.7 \text{ mm} \times 0.5 \text{ mm}$.

Pictures like in Fig.1 are present in the literature [7]. However in some of those cases, one also observes few strength $1/2$ defects, i.e. points from which only two brushes emanate. We do not get any of these. Even if we miss any such points due to resolution of the picture, it will generally lead to conflict in director assignment on the two sides of the brush following our technique (which is explained below); as we have verified from the pictures in the literature. One still needs to address the issue why there are very few strength $1/2$ defects even in the pictures such as in ref. [7], (and none in our pictures). One possibility could be that we are observing point monopole defects. However, it is known that monopole production in this manner should be highly suppressed [9]. Further, similar pictures in the literature [7] show some strength $1/2$ defects as well, which is not possible if these are monopole defects. The anchoring of the director at the I-N interface [10] forces the director to lie on a cone, with the half angle equal to about 64° . This forces the order parameter space

there to become effectively a circle S^1 , instead of being RP^2 , with the order parameter being an angle θ varying between 0 and 2π . Only defects allowed now are with integer winding and no $1/2$ windings can occur. Of course this does not imply that strength half defects should be completely forbidden. Depending on the anchoring energy, strength $1/2$ defects should be able to form, with certain region having higher energy. Normal anchoring of director at the nematic-air interface also does not allow strength $1/2$ defect at the interface. The order parameter space now is S^1 , with the space effectively being two dimensional since integer windings can be trivialized as one moves away from the I-N interface. (In this sense, these defects may be like partial monopole configurations.) Therefore the calculations for σ in Eq.(1) is valid for this case with the picture that a domain structure near the I-N interface is responsible for the formation of integer windings.

We now explain our procedure for analyzing the pictures such as in Fig.1. We assume any one of the defects (chosen randomly) to be a defect with winding plus one. (If it had minus one winding, it will only interchange all defects and antidefects, without affecting any of our calculations.) One of the brushes is then assumed to correspond to director being parallel to \vec{E} with θ assumed to be equal to zero. Assumption of plus winding then implies that the next brush, going anti-clockwise around the defect, should correspond to $\theta = \pi/2$ with the director perpendicular to \vec{E} . The next two brushes will then correspond to $\theta = \pi$, and $3\pi/2$ respectively. We now denote the first quadrant on the circle S^1 , between $\theta = 0$ and $\theta = \pi/2$ by number 1, the second quadrant, between $\theta = \pi/2$ and π by number 2, and similarly, the third and fourth quadrants by numbers 3, and 4 respectively. This allows us to write numbers 1-4 in between the brushes.

Using continuity of the order parameter outside the location of defects, one can easily see that θ in between any two brushes remains in the same quadrant irrespective of the size and the shape of that region. This is because a change of quadrant should happen only across a dark brush. In case any brush is missed due to experimental resolution, our technique will lead to conflicting assignments of quadrant number in some region when one approaches that region from different directions. We never find that to be the case. Around any defect, if we know the quadrant numbering of any two adjacent regions between the brushes, then the quadrant numbers for the remaining two regions are assigned assuming the same sense for the winding as determined by the first two quadrant numbers (this is in the spirit of the geodesic rule as explained above).

This completes the explanation of the procedure to determine θ distribution (or, rather, quadrant distribution) in a given photograph. An example is shown in Fig.2 where, following these rules, quadrant assignment is completed, starting by assuming the defect (denoted by **d**) to have +1 winding. Note that whenever two (or more) brushes join defects, they represent defect-antidefect pairs. [In between two defects of same windings there must be a region belonging to same quadrant extending to infinity, unless truncated by other defects [11].] Fig.1 shows that defect-antidefect pairs are most abundant, supporting the correlation in defect-antidefect production.

For different parts in the bottom picture in Fig.1, which represent very different average inter-defect separations (possibly due to inhomogeneity in physical conditions, such as temperature etc.) we determine the average (triangular) domain size (ξ) for these parts by taking $n_t = A/(\sqrt{3}\xi^2)$. A value of L/ξ is then determined which corresponds to aver-

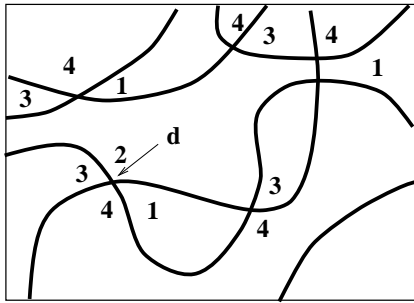


FIG. 2. Procedure for determining quadrant number for θ in regions between the brushes (represented by thick lines).

age value of $n_t = 10$. n_t is chosen small to get reasonable statistics. (We mention here that due to exponent $1/4$ of n_t , functional dependence of σ on n_t is difficult to check, as that requires very large statistics. Thus we check σ for $n_t = 10$ and distinguish between scenario of Kibble mechanism and that of uncorrelated production.) We first divide the entire picture in non-overlapping regions of square shape (for convenience), all with the same value of L/ξ . Regions are marked without noticing presence of defects to avoid any bias. The regions where defects could not be resolved/observed due to picture quality, or which formed disconnected sectors, in the sense that our procedure could not be used to determine quadrant distributions, were excluded. [Since we determine defects and antidefects only up to an overall sign, we do not combine distributions from different pictures.] In order to increase statistics, we also considered some square regions with partial overlap. It should be clear that net windings along the perimeters of such squares also represent independent statistics. In some cases when defects were touching the boundary of the square region, we take some fixed rule, for example to always include them in the square. For each square, net winding ΔN along its perimeter, (which is the same as number of defects minus number of antidefects), was determined and frequency of a given value of ΔN was plotted with respect to ΔN . Fig.3 shows the experimental points. A Gaussian was fitted to these points. Width of this Gaussian is the experimental value of σ . We repeat the entire procedure on the same picture two more times by choosing entirely new set of square regions. This leads to the following experimental value of the width σ .

$$\sigma = 1.19 \pm 0.04 \quad (2)$$

This should be compared to the theoretical prediction of $\sigma = 1.02$ from Eq.(1) for $n_t = 10$. When one takes square shaped elementary domains, predicted value of σ is 1.26 (for $n_t = 10$), which is in excellent agreement with the measured value. Defect-antidefect symmetry implies that the Gaussian should be centered at zero. The center of the fitted Gaussian is at $\Delta N \simeq 0.03$ in Fig.3. Average position of the center of the Gaussian is found to be about 0.09, which is indeed very small.

This agreement with the predicted value is quite impressive. For comparison we show, in Fig.3, the Gaussian, determined numerically (for $n_t = 10$), for the case when defects and antidefects are uncorrelated. Width of this Gaussian is 3.1 which is markedly different from the value experimentally observed. This clearly rules out any mechanism of

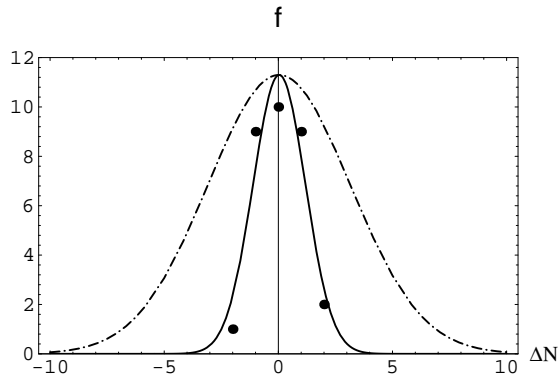


FIG. 3. Plot of the frequency of ΔN vs. ΔN . Solid dots show experimental points. Solid curve shows Gaussian fit to these points. Dashed curve shows numerically determined Gaussian when defects and antidefects are randomly distributed.

defect production where defects and antidefects are independently produced. Note that if defect-antidefect pairs were thermally produced, then any resulting correlation could only be observed for typical inter-defect separations of order of the core size of the defect (\simeq few hundred angstroms). The inter-defect separation we observe (at the time of formation itself) is of the order of 30-40 microns.

We point out other aspects of the novel technique we have described for determining θ (or, quadrant) distribution in a picture of defect network. It is an extremely efficient technique, (and also fun to play with). It turns out to yield surprisingly consistent quadrant distribution, looking at the simplicity of the steps involved. In some of the situations where there are more than one ways to proceed, often one is able to argue that either choice is fine as the resulting defect distribution is the same. When even this is not possible to argue, we do not proceed beyond that point and exclude such regions from analysis.

We conclude by stressing that these observations amount to experimentally verifying a very crucial aspect of the Kibble mechanism, namely the correlation between defects and antidefects. Another point is that the prediction of defect density crucially requires the knowledge of the domain size [5]. In ref. [2], the transition proceeded by bubble nucleations, so domains were easily identified. When domains are not that clearly identifiable, as in the present case, then how does one determine the process underlying the defect production? Here, by checking a qualitatively different aspect of the Kibble mechanism, one is able to say that the correlations in defect-antidefect production support the underlying picture being that of the Kibble mechanism. It is clear that these correlations will lead to a non-trivial behavior for density-density correlations of defects. For example, the probability of finding antidefects will show oscillatory behavior as a function of separation from a defect. All this analysis, as also, improved errors for σ in Eq.(2), requires large statistics. We will present such analysis in a future work.

We are very thankful to Supratim Sengupta for useful discussions and comments. We would like to acknowledge V.S. Ramamurthy for his encouragement and help in setting up liquid crystal experiments at IOP.

REFERENCES

- [1] T.W.B. Kibble, J. Phys. **A9**, 1387 (1976).
- [2] M.J. Bowick, L. Chandar, E.A. Schiff and A.M. Srivastava, Science 263 (1994)943.
- [3] I. Chuang, R. Durrer, N. Turok and B. Yurke, Science 251 (1991)1336.
- [4] P.C. Hendry, N.S. Lawson, R.A.M. Lee, P.V.E. McClintock, and C.D.H. Williams, J. Low. Temp. Phys. 93 (1993)1059; G.E. Volovik, Czech. J. Phys. 46 (1996) 3048 Suppl. S6.
- [5] W.H. Zurek, Phys. Rep. **276**, 177 (1996).
- [6] T. Vachaspati and A. Vilenkin, Phys. Rev. D**30**, 2036 (1984).
- [7] S. Chandrasekhar and G.S. Ranganath, Adv. Phys. **35**, 507 (1986).
- [8] W.F. Brinkman and P.E. Cladis, Phys. Today, **35**, 48 (1982).
- [9] M. Hindmarsh, Phys. Rev. Lett. **75**, 2502 (1995).
- [10] S. Faetti and V. Palleschi, Phys. Rev. **A30**, 3241 (1984).
- [11] C. Rosenzweig and A.M. Srivastava, Phys. Rev. **D43**, 4029 (1991).